Earthquakes and Structures, *Vol. 11, No. 2 (2016) 281-295*
DOI: http://dx.doi.org/10.12989/eas.2016.11.2.281

Seismic behavior of non-seismically designed reinforced concrete frame structure

Xuan-Huy Nguyen[*1,2] and Huy Cuong Nguyen[1a]

[1]*Department of Civil Engineering, University of Transport and Communications, Vietnam*
[2]*Research and Application Center for Technology in Civil Engineering, University of Transport and Communications, Vietnam*

(Received November 8, 2015, Revised July 19, 2016, Accepted July 20, 2016)

Abstract. This paper presents a study on a non-seismically designed reinforced concrete (RC) frame structure. The structure was a existing three-story office building constructed according to the 1990s practice in Vietnam. The 1/3 scaled down versions of structure was tested on a shake table to investigate the seismic performance of this type of construction. It was found that the inter-story drift and the overall behavior of structure meet the requirements of the actual seismic design codes. Then, nonlinear time history analyses are carried out using the fiber beam- column elements. The comparison between the experimental and simulation results shows the performance of the time history analysis models.

Keywords: seismic; reinforced concrete; non seismically designed; fiber beam; nonlinear; frame structure

1. Introduction

Vietnam is located in the Eurasian Plate close to the Andaman-Sumatra-Myanma plate boundary. Even in the Southeast Asia, which was usually believed to be safe against seismic hazard, the research in this issue has gained more attention (Wen *et al*. 2015, Itthi *et al*. 2011, Su 2008, Ngo *et al*. 2008, Petersen *et al*. 2007) due to several recent earthquakes in this region. Most recently, the earthquake on 24 March 2011 near the border of Myanmar, Thailand and Laos, recorded at 8.6 on the Richter scale, caused violent shaking of many buildings in the North-Western of Vietnam. It was the strongest seismic event on Southeast Asia peninsular since the December 2004 Sumatra Andaman earthquake (Mw=9.2). The tremor could be felt in high-rise building as far as in Hanoi, Vietnam. However, there are a large number of buildings in Vietnam are designed following out-of-date seismic design codes (or to non-seismic codes) because Vietnam has not had its own earthquake code before 2006. In most of these structures, the uncertainties about the nonlinear behavior are relevant: the presence and location of potential inelastic zones, the ductility capacity, are not known. In 2006, the Ministry of Construction issued the first Vietnamese earthquake loading standard TCXDVN 375:2006 (now TCVN 9386-1: 2012)

*Corresponding author, Associate Professor, E-mail: nguyenxuanhuy@utc.edu.vn
[a]Ph.D. Student, E-mail: nguyenhuycuong@utc.edu.vn

 ISSN: 2092-7614 (Print), 2092-7622 (Online)

which was based on Eurocode 8.

The objective of this study is to acquire a better understanding of the seismic performance and failure mechanisms of a non-seismically designed reinforced concrete frame structure (Bo *et al*. 2015, Tastani *et al*. 2013). The specimen, composed of three stories and one bay, is the one-third scaled model of an existing office building constructed during the 1990s in Vietnam. The first part of this paper presents the seismic responses and the failure mechanism of the structure subjected to a series of earthquake base excitations on the shaking table. The test results demonstrate that the inter-story drift and the overall behavior meet the requirements of the newest Vietnamese earthquake loading standard TCVN 9386-1: 2012. At the design level, some visible damages appeared at the joint and one reinforcement bar was finally broken. However, this local failure did not influence significantly the performance of the specimen, which was able to resist to the higher levels of loading. The second part of the paper introduces the numerical analysis using the fiber beam- column element to simulate the seismic behavior of RC frame structures. The simulation result is compared with the experimental result to estimate the performance of the time history analysis models in term of nonlinear structural characteristics, deformability, stiffness degradation and failure mechanism.

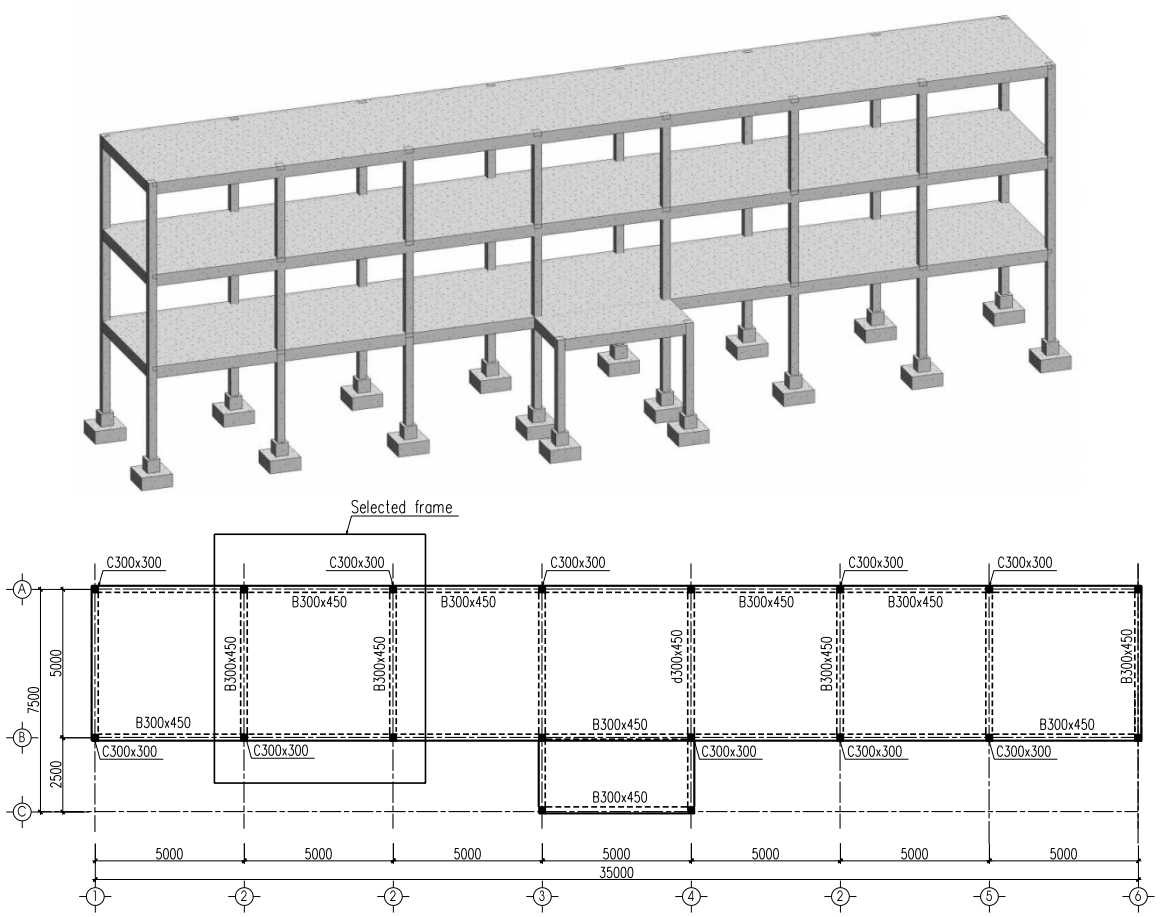

Fig. 1 The prototype building and selected test frame (unit in mm)

2. Experimental investigation

2.1 Description of structure

The tested frame structure is the model of an office building constructed during the 1990s in Vietnam. The plan view of the building and the elevation view of the frame are presented in Fig. 1. The dimensions of columns and beams of the prototype frame are 300×300 mm and 450×300 mm, respectively.

Due to the limited space of the laboratory as well as the limitations of the dimension (2 m×2 m) of shaking table, the scale factor of 1/3 was used for the test structure. Applying the similitude rules related to the conservation of acceleration for the scale model, the experiment was run with the following choices:

- The cross section of columns and beams were 100×100 mm and 150×100 mm, respectively.
- The height of each story was equal to 1 m. Hence, the total height of the specimen was 3 m.
- The thickness of the slabs of each story was equal to 5 cm.
- The total mass was about 8220 kgf which included 4400 kgf for specimen, 3600 kgf for additional masses, and 220 kgf for footing.
- Accelerations were preserved.
- Time was divided by $\sqrt{3} \approx 1.732$.

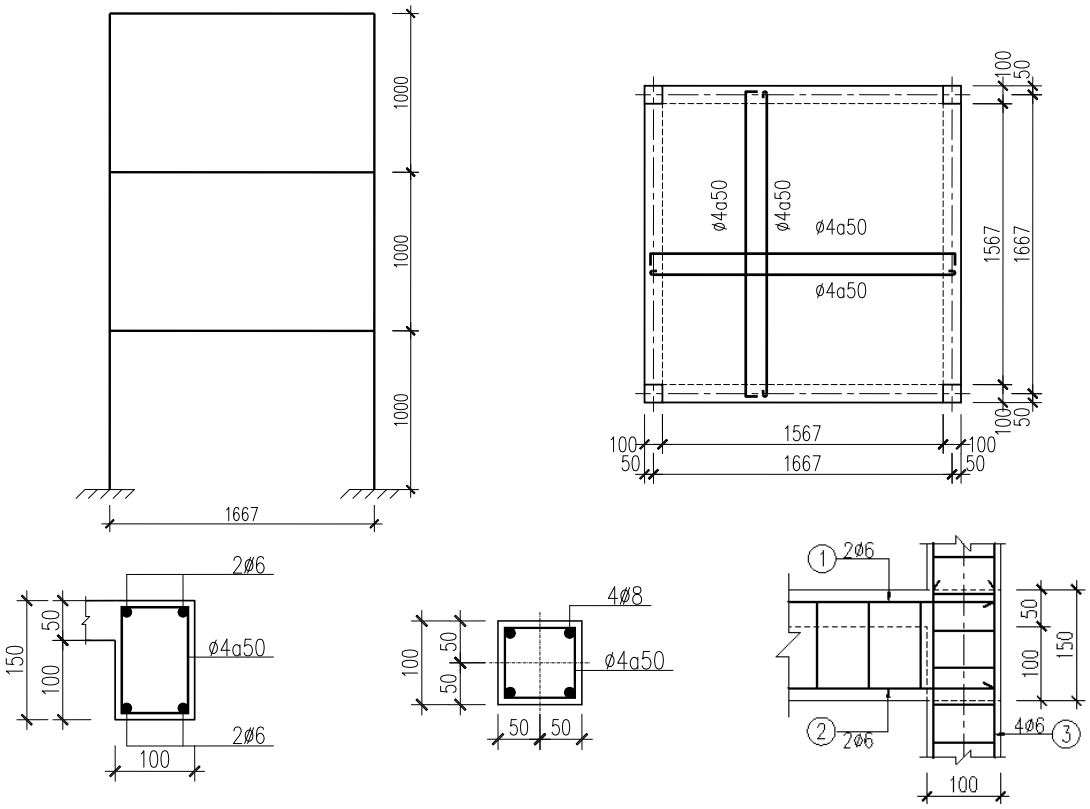

Fig. 2 Reinforcement details of test structure (unit in mm)

The yield strength of reinforcement bars was 300 MPa, 500 MPa, and 240 MPa for 6 mm, 8 mm, and 4 mm bars, respectively. The average concrete compressive strengths were 30.9 MPa.

Reinforcement detailing was specified according to TCVN 5574-91. More specifically, the test structure was characterized by the use of plain round bars, 180-degree end hooks on beam bars anchorage, widely spaced ties in the beam, lack of shear stirrups in the joint, column steel lap spliced immediately above the slab level. Details of reinforcement configuration of specimen are shown in Fig. 2.

2.2 Instrumentation layout and Input motion

The measuring devices were placed on the model so that both global and local responses of structure could be measured, including accelerations measured by accelerometers, displacements measured by LVDTs and strains measured by strain gauges. For instance, nine accelerometers were placed randomly around the joints between beams and columns. Three LVDTs were concentrated at floor levels. Twelve strain gauges were placed on columns, beams and joint sections. The overall view of the specimen on the shaking table and the installation of measuring devices are shown in Fig. 3.

Before starting of the experimental program, three sine sweep tests, denoted by TN1, TN2, and TN3, were conducted on the structure with the peak ground acceleration of 0.05 g, 0.075 g and 0.1 g in X direction, respectively. Then, the specimen was subjected to different levels of excitation. The input signals have been derived from TCVN 9386-1: 2012 spectra, soil type B, corresponding to the Tolmezzo earthquake. Six earthquake motions (denoted from TN4 to TN9) were used for the experiments with maximum acceleration increased from 0.05 g to 0.8 g. (0.05 g, 0.1g , 0.2 g, 0.4 g, 0.6 g, 0.8 g).

Summary of applied progressive ground acceleration is presented in Fig. 4.

Fig. 3 The specimen and the installation of measuring devices

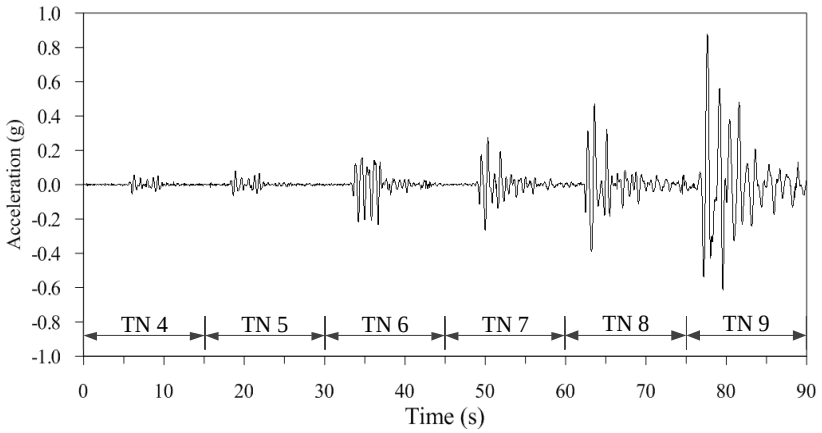

Fig. 4 Selected ground acceleration

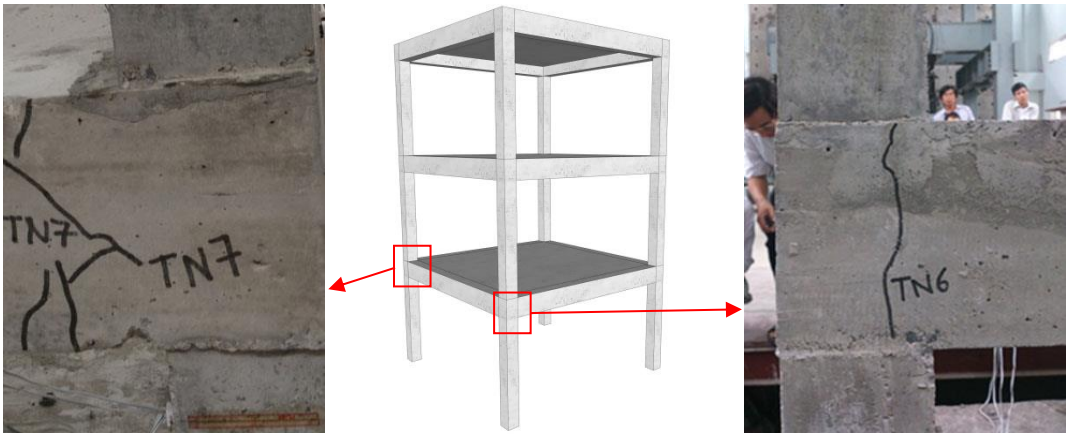

Fig. 5 The state of specimen after TN7 test

2.3 Experimental results

Sine sweep tests were conducted in two orthogonal horizontal directions in order to determine the frequency of the structure with added mass. It was found that the first 2 natural frequencies of this structure are 7.91 Hz and 23.79 Hz in flexion. However, no crack pattern was observed during three sine sweep tests (TN1, TN2, TN3).

From the test TN4 to TN9, the experimental observations of the specimen could be resumed follows: The first visible damage was flexural cracks appeared in joints of the first floor at TN6. As the testing progressed, these cracks extended gradually in this region and became significant during the test TN7. There were also some horizontal cracks at the base of the column. At the end of beam of the first floor, one transverse steel bars was broken. However, this local failure did not influence significantly the performance of the specimen, which was able to resist to much more important levels of loading.

Another cracks were developed at the base of the column during the test TN8. Moreover, some cracks were opened and concrete was crushed at the end of beam.

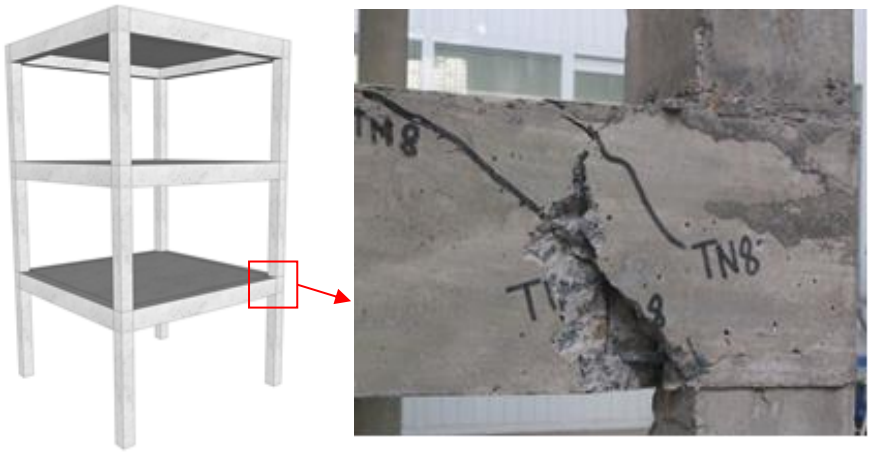

Fig. 6 The state of specimen after TN8 test

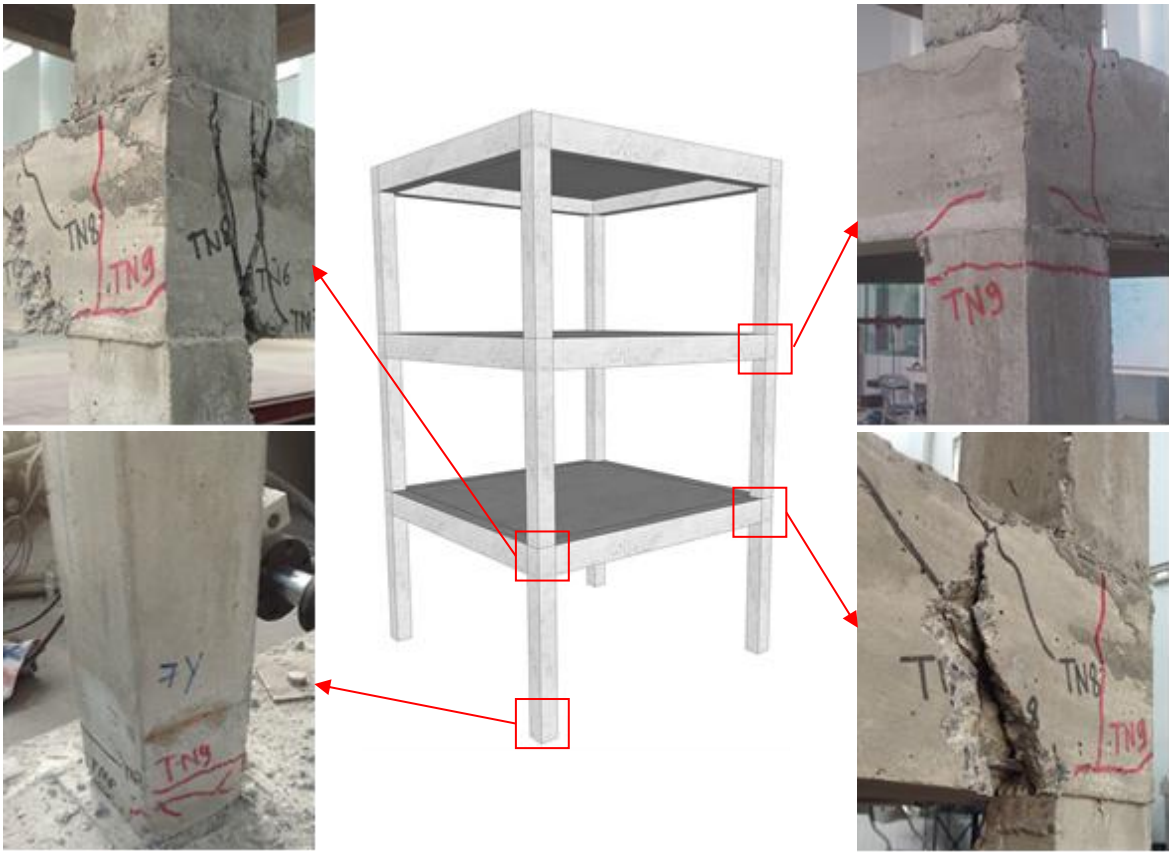

Fig. 7 The state of specimen after TN9 test

The loss of concrete cover was observed at both ends of beam in TN9 (Fig. 7). It was noted that new visible cracks were found in the joint between the second floor and the base of the column at

Table 1 Experimental results- Maximum values

Test	TN4	TN5	TN6	TN7	TN8	TN9
Displacement at the top (mm)	0.85	1.08	2.97	3.35	7.66	23.54
Acceleration at the top (m/s^2)	-1.59	-2.12	-3.70	-5.73	-9.16	14.29
Shear force at base (kN)	0.71	1.08	2.97	6.37	12.91	23.59
Drift ratio	0.0006	0.0007	0.0021	0.0023	0.0054	0.0181

this final test.

No observable damage was produced by the presence of the lapped splices in the column, indicating this detail was not critical for structure. The failure of specimen was the result of the lack of ties in the joint and widely ties in the end of beam which accentuated the cracking propagation described above.

The results of tests carried out are given in Table 1.

3. Numerical investigation

3.1 Fiber beam-column element

The nonlinear analysis of RC structures under dynamic loadings requires intensive computation. By using the fiber beam- column element, the computational effort can be reduced effectively, because it can combine the advantages of beam-type finite elements (FE) and the simplicity of uniaxial behavior (Kostic *et al*. 2011, Martinelli *et al*. 2013, Nguyen 2014). Different fibers made of different materials, such as concrete or steel, can be modeled by using the appropriate constitutive laws.

A numerical investigation using the fiber beam- column element in OpenSees software is presented below. The three-dimensional model is developed to simulate the inelastic response of the three-story RC frame for the purpose of FE validation.

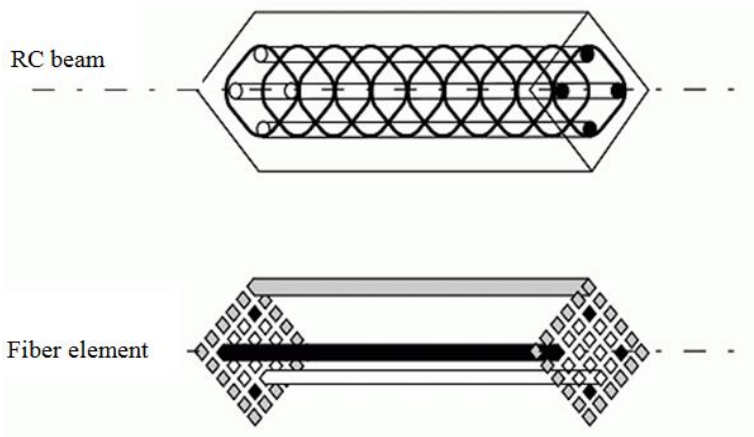

Fig. 8 Fiber element for RC structures

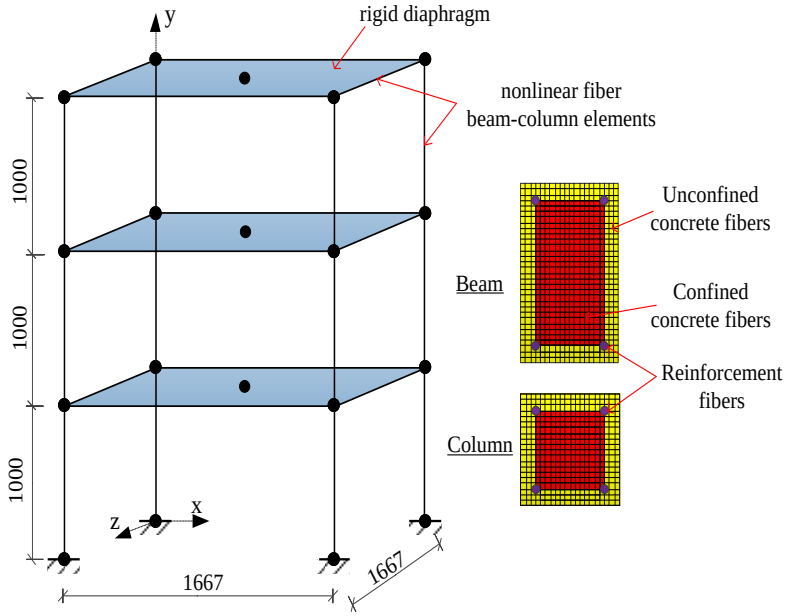

Fig. 9 Finite elements mesh

As illustrated in Fig. 9, all beams and columns of specimen were modeled as nonlinear fiber beam/column elements based on the force method formulation in which it was unnecessary to define the plastic hinge length. In this model, the flexibility distribution along the member axis was assumed to be linear, which can be formulated by flexibility matrix relationship between two end sections. Then, the analytical integration was used for calculating the member flexibility matrix instead of numerical integration to reduce the computational effort. The beam-to-column connections were fully constrained in the numerical model. Each element was divided into five segments along the element axis. The section of the column and the beam at each element was divided into 676 and 936 fibers, respectively. The fine mesh with size from 3 mm to 4 mm was chosen.

It was assumed that the nonlinear beam/column element had perfect bond between the concrete and reinforcement. The characteristics of concrete and reinforced material were the same as those of the experiment. Besides, it was reasonable to model the slabs by using the rigid diaphragm assumption because the RC slabs remained elastic.

The 3D frame structure was then exposed to two sequences of loading in the following order: gravity load, and earthquake load. The dynamic time-history loads in direction X were applied uniformly at the base of the structure. All the base nodes are considered as fully restrained against rotations and translations in order to reproduce the anchorage between the structure and the shaking table.

3.2 Constitutive models

The nonlinear analysis of RC structures under dynamic loadings requires intensive computation. By using the fiber beam- column element, the computational effort can be reduced

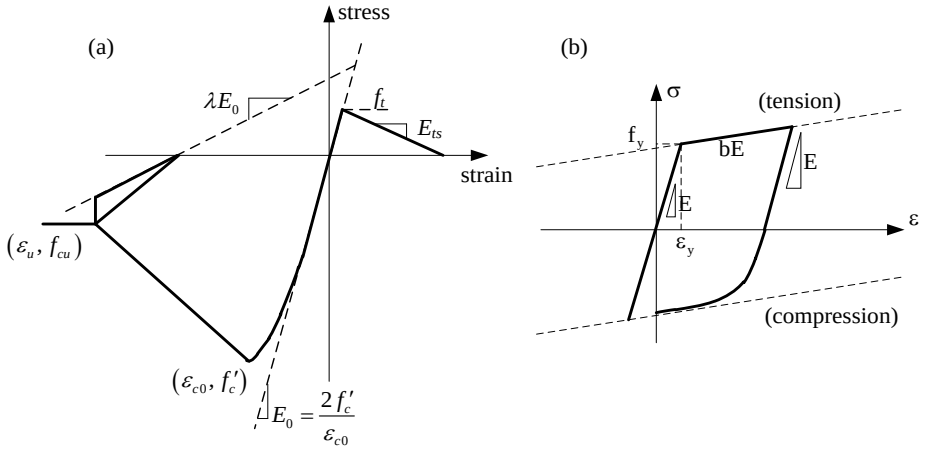

Fig. 10 Material model. (a) Concrete; and (b) Reinforcement

effectively, because it can combine the advantages of beam-type finite elements (FE) and the simplicity of uniaxial behavior. Different fibers made of different materials, such as concrete or steel, can be modeled by using the appropriate constitutive laws.

The Concrete02 model, developed by Kent-Park (Kent and Park 1971), available in OpenSees material library is used to model the concrete material. For modeling the concrete in compression, this model uses an ascending second-degree parabolic curve and a descending linear branch (see Fig. 10(a)). The parameters defining the concrete model for compression state are the concrete compressive strength (f'_c), the concrete crushing strength (f_{cu}), the concrete strain at maximum strength (ε_0), the concrete strain at crushing strength (ε_{cu}), and the ratio between unloading slope at ε_{cu} and initial slope (λ). The initial slope of the model is $E_0 = 2f_c'/\varepsilon_0$. For concrete in tension, the tensile stress was assumed to increase linearly with respect to the strain until the concrete crack occurs. The tensile strength (f_t), and tension-softening stiffness (E_{ts}) was used in this model. The core concrete is confined by the action of the hoops, and the properties of the core concrete are calculated based on the Kent-Park models.

The longitudinal steel is uniformly distributed in the corners of column, with a steel fiber defined for each individual longitudinal bar. The steel material model has a significant impact on the calculated cyclic response of the column elements. The Steel02 material model is defined using the Giuffre-Menegotto-Pinto (Menegotto *et al*. 1973) uniaxial strain-hardening material model. The model has a bilinear backbone curve with a post-yield stiffness expressed as a fraction of the initial stiffness (Fig. 10(b)). The parameters are used for defining the reinforcing steel model are the yield strength of reinforcing bar (f_y), the modulus of elasticity of steel (E_s), and the strain-hardening ratio (b). The model accounts for the Bauschinger effect, which contributes to the gradual stiffness degradation of reinforced concrete members under cyclic response. Including the Bauschinger effect gives the model a more realistic estimate of energy dissipation during cyclic loading.

3.2 Distribution of masses

In fact, the mass is distributed throughout the building. However, in this simulation, it is

idealized as the concentrated mass at the nodes or beam-column intersections. The additional masses on top of the slabs are represented in the structure by the lumped nodes and then automatically converted to gravity loads.

3.3 Numerical strategy

Damping properties of the analytical models are usually idealized using Rayleigh damping. The Rayleigh damping matrix is computed as a linear combination of the mass and stiffness matrices. The damping matrix was formed at each analytical step using the current tangent stiffness matrix and/or mass matrix. The typical damping ratio used for designing reinforced concrete structures is from 2% to 7%. In this work, the ratio is 5%, which is the most widely used value in building codes. The Newton-Raphson analysis algorithm is used to analyze the nonlinear dynamic of the model. In this strategy, the tangent stiffness is calculated for every iteration at a given increment. This strategy yields a quadratic convergence, which helps the iteration process converges after a few iterations.

4. Comparison between measured and calculated responses

4.1 Modal analysis

In order to validate the modeling assumptions, the modal analyses were performed. Elastic material properties were used for the specimen. For instance, the Young's modulus of concrete and steel reinforcement are equal to 45 MPa and 460 MPa, respectively. Table 1 shows the comparison between the simulation and experimental results in term of the first three natural frequencies of the structure. The frequencies predicted by the simulation are approximate to the measured values in the experiment.

4.2 Global responses

All six signals TN4-TN9 are applied to the specimen in chronological order. They have been launched independently in the model. Fig. 11 shows the comparison of the horizontal displacements at the top of the structure in all the tests TN4-TN9. As can be seen, the simulation results are generally close to the experimental results. No significant shift exists between the simulation and experimental curves.

The slabs' displacements in experiments TN4-TN9 are correctly estimated as shown in Fig. 12.

The inter-story drift a ratio given in Fig. 13 shows clearly that the non-linearity of the structure is concentrated at the first floor.

Table 2 Frequency and modes of the structure

Modes	Simulation	Experiment	Shape
1	7.91 Hz	8.1 Hz	Flexion
2	23.79 Hz	22.8 Hz	Flexion
3	37.66 Hz	40 Hz	Torsion

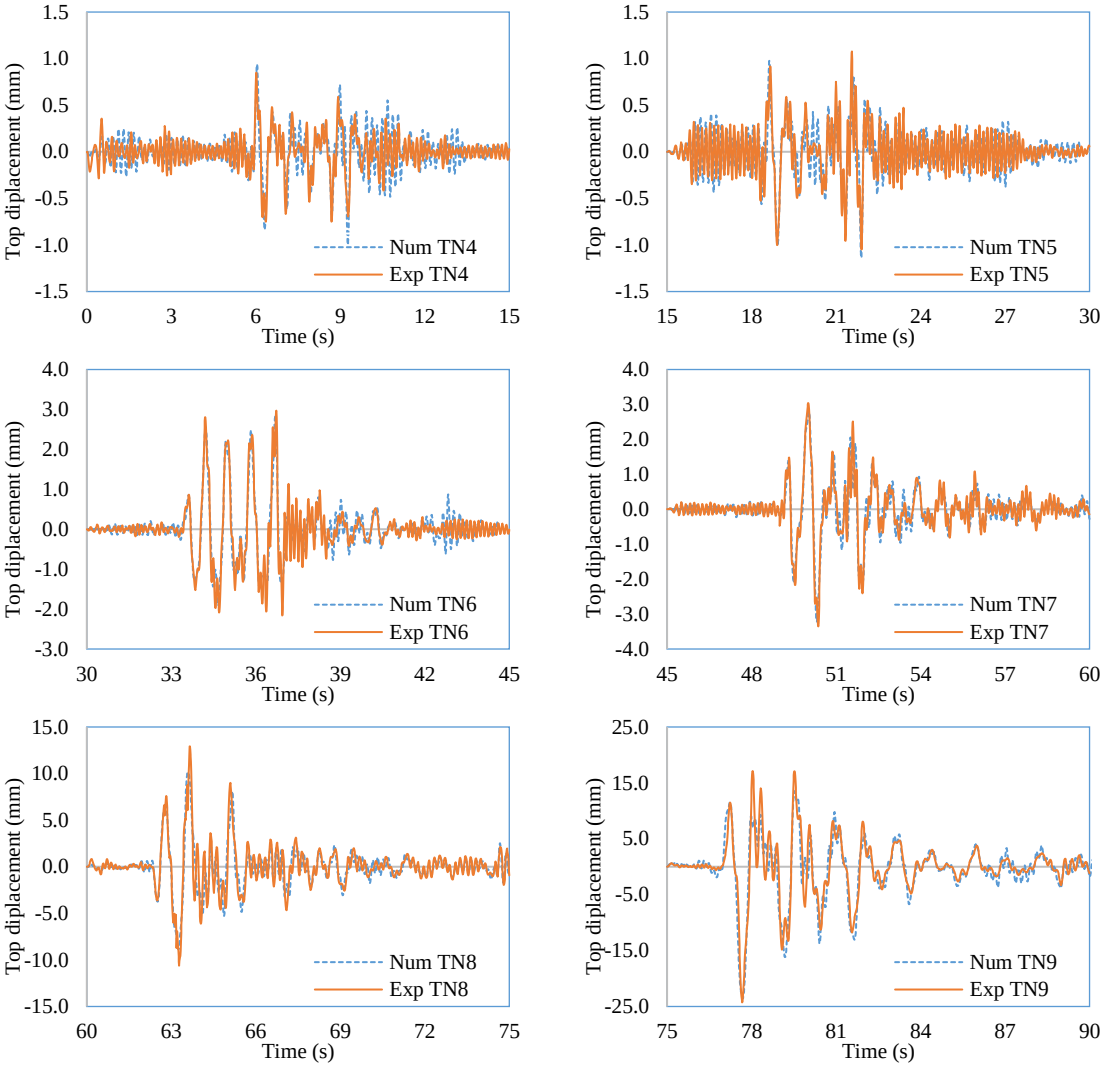

Fig. 11 Comparison of experimental and simulation displacements at the top of the structure under input motions TN4-TN9

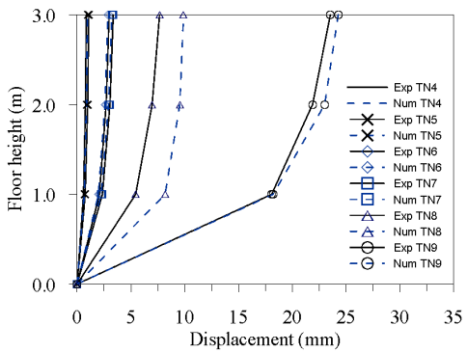

Fig. 12 Comparison of the slabs' displacement

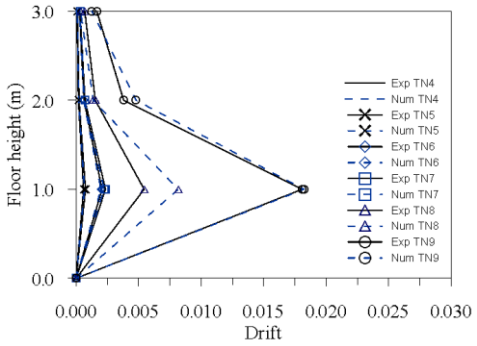

Fig. 13 Comparison of the inter-story drift ratios

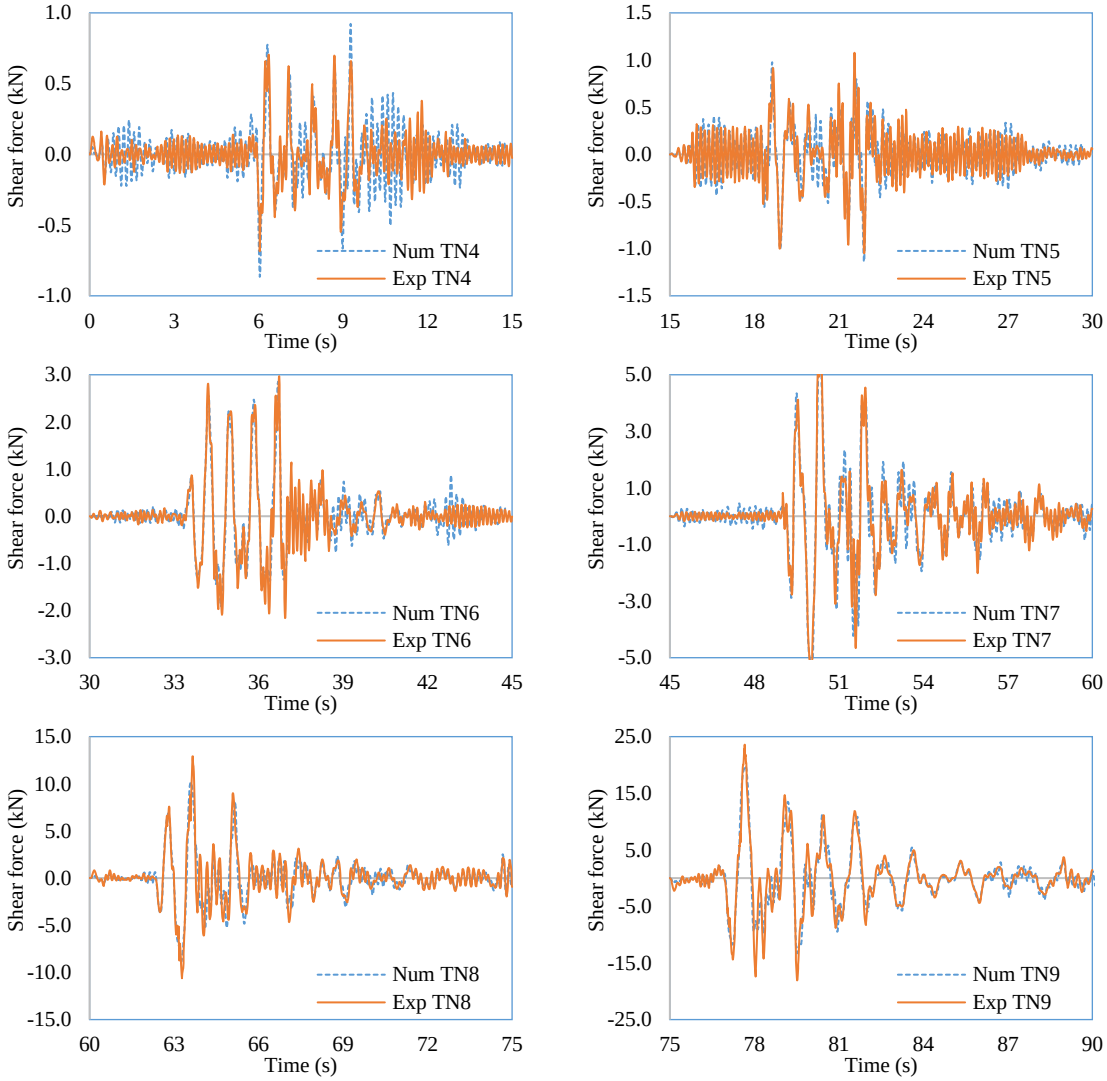

Fig. 14 Comparison of the shear forces

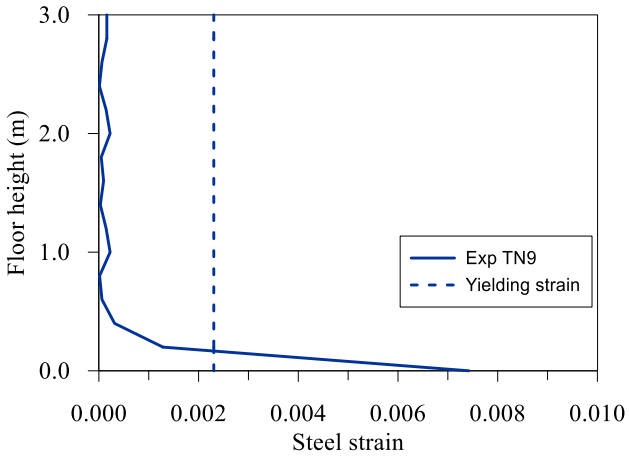

Fig. 15 State of damage after test TN9

The time histories of the shear force at the base of the structure are shown in Fig. 14. In TN4, TN5, TN6 and TN7, simulation satisfactorily predicts the behavior. In TN8 and TN9, the maximum shear force at the base is underestimated. This difference probably comes from the fact that the cracks became significant during the TN5 test so that the above assumptions are not correct any more. In the other words, the slab stiffness is overestimated when using the joint constraints between column top nodes and the rigid diaphragm in X-Y plane for each floor level in TN5 and TN6.

4.2 Local responses

For a more accurate assessment of the capability of the numerical model to describe the failure pattern evolution of the test specimen during the six input motions of increasing intensity, the local damage (in the concrete and in the reinforcing steel) is compared. Fig. 15 shows the envelope of steel strains in a reinforcing fiber along the height of the column after the TN9. At the base, strains are greater than 0.22% (dotted line- value corresponding approximately to the yielding strain of the longitudinal reinforcement). The simulation predicts rupture of the reinforcing steel at the TN9. Furthermore, significant compressive strains occurring at the joints of first floor (0.85%) indicate that concrete may be collapsed from this location due to excessive strains. This is in accordance with the local behavior observed in the experiment.

5. Conclusions

This paper presents a study on a non-seismically designed RC frame structure which was a existing building constructed according to the 1990s practice in Vietnam. The specimen was 1/3 scaled down and subjected to six consecutive table motions with increasing maximum acceleration from 0.1 g to 0.8 g. A simplified numerical investigation utilizing the fiber beam-column elements is chosen to simulate the seismic behavior of the structure. The following conclusions and recommendations can be drawn from this study:

• Following the TCVN 9386-1:2012 code, the design loading of this type of structure is 0.21 g which is smaller than the peak ground acceleration (0.27 g) of TN7. It is could be concluded that the present structure is able to resist to the higher level of peak ground acceleration in comparison with the design loading.

• The lack of ties in the joint and widely ties in the end of beam have accentuated failure process of the test structure.

• The numerical model successfully simulated the global behavior of the structure in term of the natural periods of the structure, the inter-story drift ratio, the time histories of the shear force at the base of the structure, and the horizontal displacements at the top of the structure; except for the maximum values of the shear force in TN8 and TN9. Following the simulation results, the main damages are in accordance with the local behavior observed in the experiment.

• The results indicated that the level of discretization and the type of numerical elements adopted in the model were sufficient to predict the non-linear behavior of the RC structures under dynamic loadings with a good compromise among the computation cost, the quality of results and the facility of modeling. This proposed numerical modeling strategy may be used to further investigate the nonlinear dynamic responses of a variety of structures.

References

Bo, L., Eddie, L., Yuk-kit, C., Bo, W. and Ya-yong, W. (2015), "Strengthening of non-seismically designed beam-column joints by ferrocement jackets with chamfers", *Earthq. Struct.*, **8**(5), 1017-1038.

Ile, N., Nguyen, X.H., Mazars, J., Kotronis, P. and Reynouard, J.M. (2008), "Shaking table tests of lightly RC walls: numerical simulation", *J. Earthq. Eng.*, **12**(6), 849-878.

Itthi, T., Andy, H. and Anuphao, A. (2011), "Co-Seismic displacement of 24 March 2011MW=6.8 Mong Hpayak earthquake, Myanmar", *Proceding 'Fringe 2011Workshop'*, Frascati, Italy.

Kent, D.C. and Park, R. (1971), "Flexural members with confined concrete", *J. Struct. Div.*, **97**(7), 1969-1990.

Kostic, S. and Filippou, F. (2012), "Section discretization of fiber beam-column elements for cyclic inelastic response", *J. Struct. Eng*., **138**(5), 592-601.

Martinelli, L., Martinelli, P. and Mulas, G. (2013), "Performance of fiber beam-column elements in the seismic analysis of a lightly reinforced shear wall", *Eng. Struct.*, **49**, 345-359.

Menegotto, M. and Pinto, P.E. (1973), "Method of anaysis for cyclically loaded reinforced concrete plane frames including changes in geometry and non-elastic behavior of elements under combined normal force and bending", *Proceeding of the IABSE Symp. of Resistance and Ultimate Deformability of Structures Acted on by Well-Defined Repeated Loads*, International Association of Bridge and Structural Engineering, Libson, Portugal.

Ngo, T.D., Nguyen, M.D. and Nguyen, D.B. (2008), "A review of the current Vietnamese earthquake design code", *Electro. J. Struct. Eng.*, **8**(2) 32-41.

Nguyen, X.H. (2014), "Performance of multifiber beam element for seismic analysis of reinforced concrete structures", *Int. J. Struct. Stab. Dyn.*, **14**(6), 1450013.

Nguyen, X.H. and Nguyen, H.C. (2013), "Seismic behaviour of reinforced concrete frame structures", *Proceedings of The national scientific conference on Mechanical Deformation of Solid*, Ho Chi Minh city, Vietnam.

Opensees web site: opensees.berkeley.edu.

Petersen, M., Harmsen, S., Mueller, C., Haller, K., Dewey, J., Nicolas, L. and Crone, A. (2007), "Documentation for the Southeast Asia seismic hazard maps", *USGS Administrative Report*, p.28.

Su, R.K.L (2008), "Seismic behaviour of buildings with transfer structures in low-to-moderate sesimicity regions", *Electro. J. Struct. Eng.*, **8**(2), 99-109.

Tastani, S.P. and Pantazopoulou, S.J. (2013), "Yield penetration in seismically loaded anchorages: effects on member deformation capacity", *Earthq. Struct.*, **5**(5), 527-552.
TCVN 5574-91 (1991), "Vietnamese standard plain and reinforced concrete - code of practice", Ministry of Construction. (in Vietnamese)
TCVN 9386-1: 2012 (2012), Vietnamese seismic design standard, *Vietnamese Building Standard*. (in Vietnamese)
TCXD 198:1997 (1997), Design of multi-story monolithic reinforced concrete buildings, *Vietnamese Building Standard*. (in Vietnamese)
TCXDVN 375:2006 (2006), Vietnamese seismic design standard, *Vietnamese Building Standard*. (in Vietnamese)
Wen, Yanga, Jie, Liua, Jia, Chenga, Xuemei, Zhanga and Haixia, Shi (2015), "The impact of the 24 March 2011 Myanmar earthquake (MS 7.2) on seismic structure of the Yunnan region", *Tectonophys.*, **649**(9), 165-175.

KT